

## Dynamic analysis of deployable structures using independent displacement modes based on Moore-Penrose generalized inverse matrix

Ping Xiang<sup>1</sup>, Minger Wu<sup>\*2</sup> and Rui Q. Zhou<sup>3</sup>

<sup>1</sup>Department of Architecture, Waseda University, 3-4-1 Okubo, Tokyo 169-8555, Japan

<sup>2</sup>Department of Building Engineering, Tongji University, 1239 Siping Road, Shanghai 200092, China

<sup>3</sup>Shanghai Institute of Mechanical & Electrical Engineering Co., Ltd,  
1287 West Beijing Road, Shanghai 200040, China

(Received December 2, 2014, Revised January 27, 2015, Accepted April 4, 2015)

**Abstract.** Deployable structures have gained more and more applications in space and civil structures, while it takes a large amount of computational resources to analyze this kind of multibody systems using common analysis methods. This paper presents a new approach for dynamic analysis of multibody systems consisting of both rigid bars and arbitrarily shaped rigid bodies. The bars and rigid bodies are connected through their nodes by ideal pin joints, which are usually fundamental components of deployable structures. Utilizing the Moore-Penrose generalized inverse matrix, equations of motion and constraint equations of the bars and rigid bodies are formulated with nodal Cartesian coordinates as unknowns. Based on the constraint equations, the nodal displacements are expressed as linear combination of the independent modes of the rigid body displacements, i.e., the null space orthogonal basis of the constraint matrix. The proposed method has less unknowns and a simple formulation compared with common multibody dynamic methods. An analysis program for the proposed method is developed, and its validity and efficiency are investigated by analyses of several representative numerical examples, where good accuracy and efficiency are demonstrated through comparison with commercial software package ADAMS.

**Keywords:** multibody system; deployable structure; dynamic analysis; constraint equations; equations of motion; generalized inverse matrix

### 1. Introduction

Multibody dynamics describes the physics of motion of an assembly of constrained or restrained bodies. As such it encompasses the behavior of nearly every living or inanimate object in the universe (Rahnejat and Rothberg 2004). Many advances have been made in dynamic analysis of constrained multibody systems in the past several decades (e.g., Liu and Huston 2008, Gan *et al.* 2015, Yesilce 2015). With the development of computer technology, dynamic analysis of systems such as robots, space deployable structures (Fig. 1) and complex machines, can be

---

\*Corresponding author, Professor, E-mail: [wuminger@tongji.edu.cn](mailto:wuminger@tongji.edu.cn)

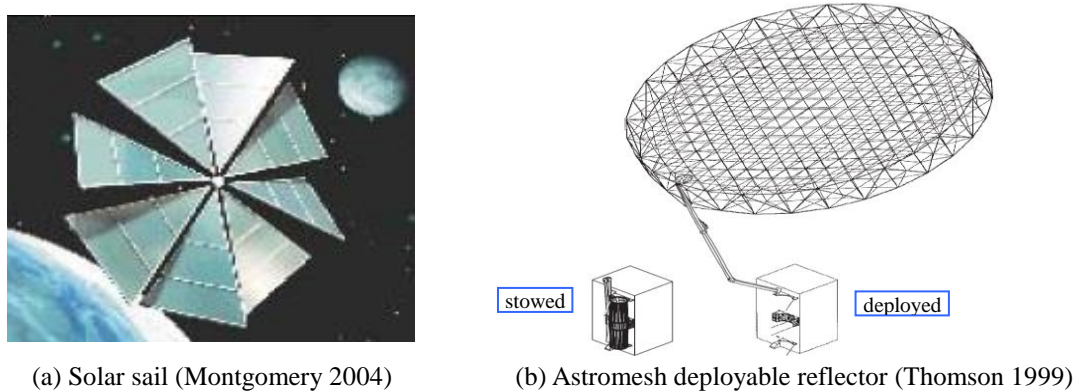


Fig. 1 Space deployable structures

accomplished using commercial software packages, such as ADAMS (MSC.ADAMS 2005), which are based on dynamics of constrained multibody systems (Ahmed 2013, Masarati *et al.* 2014).

Equations of motion and constraint equations are two fundamental types of equations employed in dynamic analysis. Newton-Euler equations are basic equations in dynamic analysis. D'Alembert's principle can be used to eliminate constraint forces in equations of motion by considering work performed by constraint forces of ideal constraints to be zero. Wittenburg (1977), Schiehlen (2007), Roberson (1988) have made a lot of progresses in multibody dynamics. Udwadia and Kalaba (2001, 2004) developed general and explicit equations of motion for systems with non-ideal constraints, in which work performed by constraint forces under virtual displacements is no longer zero.

The Lagrange multiplier method is a powerful method in which the constraints are collected into dynamic equations. Equations of motion take a form of differential-algebraic equations (DAEs). Constraint forces do not appear in the DAEs, but they can be calculated easily using Lagrange multipliers. The DAE variables include both generalized coordinates and the Lagrange multipliers, which can make the dimension of the DAEs very large. Numerical algorithms used for solving DAEs efficiently are necessary (Orlandea *et al.* 1977), and several algorithms and problems have been developed and solved (Çelik and Bayram 2004, Elsheikh 2015).

Kane (1961) used generalized velocities instead of generalized coordinates to describe motion of multibody systems. Kane's equations are established using Lagrange's form of the d'Alembert principle. No constraint reactions appear in equations of motion for either holonomic or nonholonomic constraint problems. Kane's method avoids differentiation of energy functions, which is required for the Lagrange multiplier method.

Commonly, utilizing dependent instead of independent generalized coordinates is more convenient in formulating equations of motion and constraints (Olivier and André 2008). Several efficient schemes have been suggested to find independent generalized coordinates by extracting the orthogonal complement of the Jacobian matrix (Kamman and Huston 1984, Singh and Likins 1985, Kim and Vanderploeg 1986, Ider and Amirouche 1988).

The motion of multibody systems can be described in terms of Cartesian coordinates or relative coordinates. When Cartesian coordinates are employed, motion of each rigid body is described by translation of the centroid and the rotation around the centroid. Equations of motion are obtained

by the Newton-Euler or Lagrangian mechanics using coordinates of the centroid and the rotation angles (such as Euler angles). It is straightforward to formulate motion and constraint equations with the Cartesian coordinate system, but too many equations are required since six variables (or three variables in two dimensions) are necessary to describe the motion of each body. Relative coordinates, in the form of relative rotations or relative displacements, describe the position of each body in relation to the previous body in the multibody system. The major advantage of using relative coordinates is that the resulting system has the minimum number of dependent coordinates. However, the coefficient matrix of the equations of motion is difficult to formulate.

García de Jalón *et al.* (1986, 1993, 2007) proposed a new series of Cartesian coordinates called natural coordinates. In this coordinate system, position of each body is described by the Cartesian coordinates of several selected points and unit vectors. These points include joints between bodies. Because points defined at the joints are shared by the related bodies, number of unknowns in the equations of motion is reduced.

Linked-chain systems and kinematically indeterminate framework structures have been studied in structural engineering. These types of structures are categorized as unstable structures, which are also called mechanisms or kinematically indeterminate structures. Tanaka and Hangai (1986) studied rigid body displacement modes of unstable truss structures using the generalized matrix method. Pellegrino and Calladine (1986) examined modes of inextensional deformation by analyzing subspaces of the equilibrium matrix. Hangai and Kawaguchi (1990, 1993) analyzed quasi-static displacements of link structures and extended their method to dynamic analysis. Zhao and Guan (2005) performed dynamic analysis of deployable truss structures using the generalized matrix method. Hangai and Wu (1999) formulated constraint equations of a rigid body using nodal Cartesian coordinates as unknowns and used the equations in structural analysis of a system consisting of straight elements and rigid bodies. In all of these studies, a matrix analysis method was employed in which nodal coordinates were used as variables.

In multibody systems, all the bodies are connected through joints. In many cases, positional information (i.e., coordinates, velocities and accelerations) of the joints is much more important than that of the bodies for dynamic analysis. It is straightforward to formulate equations of motion and constraints, when the Cartesian coordinates of the joints are used as unknowns, such as the natural coordinates proposed by García de Jalón (1986, 1993, 2007). In this study, a rigid body is considered as a whole, and first and second-order constraint equations of rigid body using nodal displacements as variables are derived by the generalized inverse matrix method (Hangai and Wu (1999)). The dynamic equation with nodal accelerations as variables is established at first. Then, the deploying process analysis is carried out by means of Moore-Penrose generalized inverse matrix and Newmark- $\beta$  numerical integration. This paper proposes such a new dynamic analysis method for multibody systems that has the following characteristics.

1. Multibody systems to be analyzed in this study consist of rigid bars with two nodes and arbitrarily shaped rigid bodies with more than two nodes. The bars and the rigid bodies are connected through their nodes by ideal pin joints.

2. Only the Cartesian coordinates of all the nodal points are employed as unknowns in both equations of motion and constraint equations.

3. The constraint equations for the nodal displacements of each rigid body are formulated by eliminating freedom of the centroid. This approach was firstly used in the stress-displacement analysis of hybrid structures (Hangai and Wu 1999). The Jacobian matrix is given in a generalized form, which can be straightforwardly calculated using coordinates of the nodes and the centroid of a rigid body with any number of nodes.

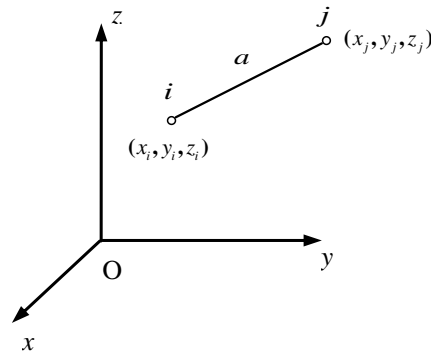


Fig. 2 Rigid bar

4. Equations of motion of the rigid bodies are based on accelerations of the nodes instead of their translational and rotational accelerations. Consequently, constraint forces between the rigid bodies are automatically eliminated when equations of motion of the multibody system are assembled.

5. Nodal displacements are transformed from dependent variables to independent variables using independent modes of the rigid body displacements calculated from constraint equations. Equations of motion are written in terms of the displacements within a short time interval and solved numerically.

In addition, an analysis program based on the proposed method is developed for multibody systems by the authors. In this paper, three representative multibody structures are analyzed using the program, and its accuracy and computational efficiency are validated by comparison between the analysis results of the proposed method and those of the commercial software package ADAMS.

## 2. Constraint equations and equations of motion

### 2.1 Rigid bar

Consider a rigid bar  $a$  with a length of  $l$  (see Fig. 2),  $i$  and  $j$  are the two end nodes of the rigid bar. Defining  $\mathbf{x}_i$  and  $\mathbf{x}_j$  to be coordinate vectors of  $i$  and  $j$ , respectively, and  $\boldsymbol{\lambda}$  to be the direction cosine vector of the bar, we have

$$l = \left[ (\mathbf{x}_j - \mathbf{x}_i)^T (\mathbf{x}_j - \mathbf{x}_i) \right]^{\frac{1}{2}} \quad (1)$$

$$\boldsymbol{\lambda} = \frac{1}{l} (\mathbf{x}_j - \mathbf{x}_i) \quad (2)$$

Let  $\mathbf{d}_i$  and  $\mathbf{d}_j$  be incremental displacement vectors of  $i$  and  $j$ , respectively, over a time increment,  $\Delta t$ . Using the first- and second-order differentials of Eq. (1) and considering that  $\dot{l} = \ddot{l} = 0$ ,  $\mathbf{d}_i = \dot{\mathbf{x}}_i \Delta t$  and  $\mathbf{d}_j = \dot{\mathbf{x}}_j \Delta t$ , the first- and second-order nodal displacement constraint equations are obtained as follows

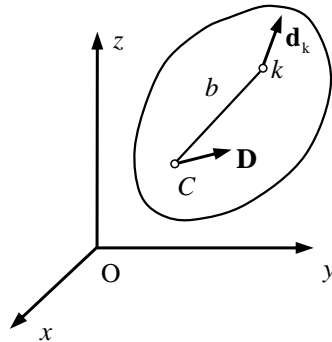


Fig. 3 Rigid body

$$\begin{Bmatrix} -\lambda^T & \lambda^T \end{Bmatrix} \begin{Bmatrix} \mathbf{d}_i \\ \mathbf{d}_j \end{Bmatrix} = \mathbf{0} \tag{3}$$

$$\begin{Bmatrix} -\lambda^T & \lambda^T \end{Bmatrix} \begin{Bmatrix} \dot{\mathbf{d}}_i \\ \dot{\mathbf{d}}_j \end{Bmatrix} + \ddot{\Phi}_a = \mathbf{0} \tag{4}$$

where  $\ddot{\Phi}_a$  can be expressed as

$$\ddot{\Phi}_a = \frac{1}{l} (\dot{\mathbf{x}}_j - \dot{\mathbf{x}}_i)^T (\dot{\mathbf{x}}_j - \dot{\mathbf{x}}_i) \Delta t \tag{5}$$

Let nodal forces of the rigid bar at  $i$  and  $j$  be  $\mathbf{f}_i$  and  $\mathbf{f}_j$ , respectively, the equations of motion for the rigid bar can be expressed as

$$\mathbf{M}_a \begin{Bmatrix} \mathbf{a}_i \\ \mathbf{a}_j \end{Bmatrix} = \begin{Bmatrix} \mathbf{f}_i \\ \mathbf{f}_j \end{Bmatrix} \tag{6}$$

where  $\mathbf{M}_a$  is the mass matrix of the rigid bar, and the acceleration vectors of  $i$  and  $j$  are respective  $\mathbf{a}_i$  and  $\mathbf{a}_j$ .  $\mathbf{M}_a$  can be constructed as a lumped mass matrix or a consistent mass matrix. The consistent mass matrix is derived by choosing the same shape functions as them used in the derivation of its stiffness matrix. For a 2-node rigid bar in 3-dimension, the stiffness shape functions are  $\mathbf{N}_a = \begin{bmatrix} \frac{1-\xi}{2} \mathbf{I} & \frac{1+\xi}{2} \mathbf{I} \end{bmatrix}$ , where  $\xi$  is the isoparametric natural coordinate that varies from -1 at node  $i$  to +1 at node  $j$ , and  $\mathbf{I}$  is a  $3 \times 3$  identity matrix. With  $dx = dy = dz = \frac{1}{2} l d\xi$ , the consistent mass matrix can be obtained as

$$\mathbf{M}_a = \int_{-1}^1 \frac{1}{2} \bar{m}_a l (\mathbf{N}_a)^T \mathbf{N}_a d\xi = \frac{1}{6} m_a \begin{bmatrix} 2\mathbf{I} & \mathbf{I} \\ \mathbf{I} & 2\mathbf{I} \end{bmatrix} \tag{7}$$

where  $\bar{m}_a$  and  $m_a$  are, respectively, the linear density and mass of the rigid bar.

## 2.2 Rigid body

Consider a rigid body  $b$  (see Fig. 3), where its centroid, i.e., the center of mass, is denoted as  $C$ , there are  $k_b$  nodes through which rigid body connects with other bars and rigid bodies. Let the displacement at the centroid  $C$  of the rigid body during time interval  $\Delta t$  be  $\{D_x D_y D_z\}^T$ , and the rotation of the rigid body with respect to the fixed reference system  $Oxyz$  during  $\Delta t$  be  $\{\Omega_x \Omega_y \Omega_z\}^T$ . The displacement  $\mathbf{d}_k$  of node  $k$  during  $\Delta t$  can then be expressed as

$$\mathbf{d}_k = \mathbf{H}_k \mathbf{D} \quad (8)$$

where

$$\mathbf{d}_k = \{d_{kx} \ d_{ky} \ d_{kz}\}^T \quad (9)$$

$$\mathbf{D} = \{D_x \ D_y \ D_z \ \Omega_x \ \Omega_y \ \Omega_z\}^T \quad (10)$$

$$\mathbf{H}_k = \begin{bmatrix} 1 & 0 & 0 & 0 & z_k - z_c & -(y_k - y_c) \\ 0 & 1 & 0 & -(z_k - z_c) & 0 & x_k - x_c \\ 0 & 0 & 1 & y_k - y_c & -(x_k - x_c) & 0 \end{bmatrix} \quad (11)$$

$\{x_k \ y_k \ z_k\}^T$  are the coordinates of node  $k$ , and  $\{x_c \ y_c \ z_c\}^T$  are the coordinates of the centroid  $C$ .

Considering all the nodes of the rigid body, Eq. (8) can be rewritten as

$$\mathbf{d}_b = \mathbf{H} \mathbf{D} \quad (12)$$

where

$$\mathbf{d}_b = \{\mathbf{d}_1; \dots; \mathbf{d}_{k_b}\} \quad (13)$$

$$\mathbf{H} = \{\mathbf{H}_1; \dots; \mathbf{H}_{k_b}\} \quad (14)$$

It should be noted that matrix  $\mathbf{H}$  in Eq. (12) is a non-square matrix. To eliminate vector  $\mathbf{D}$  in Eq. (12), the necessary and sufficient condition for Eq. (12) to have a solution is used. This condition can be expressed as (Penrose 1955)

$$[\mathbf{I} - \mathbf{H}\mathbf{H}^+] \mathbf{d}_b = \mathbf{0} \quad (15)$$

where  $\mathbf{H}^+$  is the Moore-Penrose generalized inverse matrix of  $\mathbf{H}$ . The Moore-Penrose generalized inverse can be obtained numerically by the QR factorization method, the singular value decomposition method, and so on (Ben-Israel 2003). Eq. (15) is the first-order constraint equation for the rigid body, with the nodal displacements of the rigid body as variables.

Differentiating Eq. (12) gives

$$\dot{\mathbf{d}}_b = \mathbf{H}\dot{\mathbf{D}} + \dot{\mathbf{H}}\mathbf{D} \quad (16)$$

Eq. (16) can be rearranged as

$$\mathbf{H}\dot{\mathbf{D}} = \dot{\mathbf{d}}_b - \dot{\mathbf{H}}\mathbf{D} \quad (17)$$

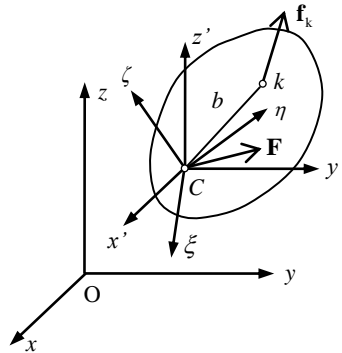


Fig. 4 Coordinate system and forces on rigid body

Likewise, using the necessary and sufficient condition for the solvability of Eq. (17), after eliminating vector  $\dot{\mathbf{D}}$ , Eq. (18) can be obtained

$$[\mathbf{I} - \mathbf{H}\mathbf{H}^+](\dot{\mathbf{d}}_b - \dot{\mathbf{H}}\mathbf{D}) = \mathbf{0} \tag{18}$$

From Eq. (12), Eq. (19) can be obtained

$$\mathbf{D} = \mathbf{H}^+ \mathbf{d}_b \tag{19}$$

Substituting Eq. (19) into Eq. (18) gives

$$[\mathbf{I} - \mathbf{H}\mathbf{H}^+]\dot{\mathbf{d}}_b + \ddot{\Phi}_b = \mathbf{0} \tag{20}$$

where

$$\ddot{\Phi}_b = -[\mathbf{I} - \mathbf{H}\mathbf{H}^+]\dot{\mathbf{H}}\mathbf{H}^+ \mathbf{d}_b \tag{21}$$

Eqs. (15) and (20) are respective the first- and second-order displacement constraint equations, with the nodal displacements during the short time interval  $\Delta t$  as variables.

Consider the motion of rigid body  $b$ . Let  $Oxyz$  be the fixed reference coordinate system,  $C\xi\eta\zeta$  be the centroid connection coordinate system of the rigid body and  $Cx'y'z'$  be the centroid translation coordinate system of the rigid body (see Fig. 4).

Consider the forces acting on the rigid body, which is connected to other bars or rigid bodies through nodes. Let  $\mathbf{F}$  be the external force vector acting on the centroid  $C$ , where  $\mathbf{F}$  consists of the force vector  $\{F_x \ F_y \ F_z\}^T$  and the moment vector  $\{M_x \ M_y \ M_z\}^T$ . Defining  $\mathbf{f}_k$  to be the external force vector acting on node  $k$ , we have

$$\begin{cases} m\ddot{D}_x = F_x + \sum_{k=1}^{k_b} f_{kx} \\ m\ddot{D}_y = F_y + \sum_{k=1}^{k_b} f_{ky} \\ m\ddot{D}_z = F_z + \sum_{k=1}^{k_b} f_{kz} \end{cases} \tag{22}$$

where  $f_{kx}$ ,  $f_{ky}$  and  $f_{kz}$  are three components of  $\mathbf{f}_k$ , and  $m$  is mass of the rigid body.

The angular momentum  $\mathbf{H}_C^O$  of the rigid body at the centroid  $C$  with respect to the fixed reference coordinate system  $Oxyz$  can be expressed as

$$\mathbf{H}_C^O = \mathbf{J}^O \boldsymbol{\omega}^O \quad (23)$$

where  $\mathbf{J}^O$  is the inertia matrix of the rigid body with respect to the centroid translation coordinate system  $Cx'y'z'$ . The value of  $\mathbf{J}^O$  changes as the rigid body rotates.  $\boldsymbol{\omega}^O$  is the angular velocity of the rigid body with respect to the fixed reference system  $Oxyz$ , and can be represented as  $\{\omega_x \ \omega_y \ \omega_z\}^T$ .

To simplify the formulation, the inertial principal axis coordinate system at the centroid  $C$  of the rigid body is used as the centroid connection coordinate system  $C\xi\eta\zeta$ , and the inertia matrix  $\mathbf{J}_C$  with respect to  $C\xi\eta\zeta$  will then be a constant diagonal matrix. Using the relationship between the inertia matrices of connected coordinate systems with the same origin,  $\mathbf{J}^O$  can be given by Eq. (24).

$$\mathbf{J}^O = \mathbf{C} \mathbf{J}_C \mathbf{C}^T \quad (24)$$

where  $\mathbf{C}$  is the direction cosine matrix of the inertial principal axis coordinate system  $C\xi\eta\zeta$  with respect to the fixed reference coordinate system  $Oxyz$ .  $\mathbf{C}$  can be expressed as

$$\mathbf{C} = \begin{bmatrix} c_{11} & c_{12} & c_{13} \\ c_{21} & c_{22} & c_{23} \\ c_{31} & c_{32} & c_{33} \end{bmatrix} = \begin{bmatrix} \cos\psi\cos\varphi - \sin\psi\cos\theta\sin\varphi & -\cos\psi\sin\varphi - \sin\psi\cos\theta\cos\varphi & \sin\psi\sin\theta \\ \sin\psi\cos\varphi + \cos\psi\cos\theta\sin\varphi & -\sin\psi\sin\varphi + \cos\psi\cos\theta\cos\varphi & -\cos\psi\sin\theta \\ \sin\theta\sin\varphi & \sin\theta\cos\varphi & \cos\theta \end{bmatrix} \quad (25)$$

$(c_{11}, c_{21}, c_{31})$ ,  $(c_{12}, c_{22}, c_{32})$  and  $(c_{13}, c_{23}, c_{33})$  are the direction cosine vector components of the inertial principal axes  $C\xi$ ,  $C\eta$  and  $C\zeta$ , respectively, with respect to the fixed reference coordinate system  $Oxyz$ , and  $\psi$ ,  $\theta$  and  $\varphi$  are the Euler angles of the inertial principal coordinate system  $C\xi\eta\zeta$  with respect to  $Oxyz$ .

Let  $\Sigma \mathbf{m}_C(\mathbf{F})$  be the total moment on the rigid body with respect to the centroid  $C$ , we have

$$\frac{d\mathbf{H}_C^O}{dt} = \Sigma \mathbf{m}_C(\mathbf{F}) \quad (26)$$

Eq. (26) is expanded into

$$\dot{\mathbf{H}}_C^O = \sum \begin{Bmatrix} m_x(\mathbf{F}) \\ m_y(\mathbf{F}) \\ m_z(\mathbf{F}) \end{Bmatrix} = \begin{Bmatrix} M_x + \sum_{k=1}^{k_b} [(y_k - y_c) f_{kz} - (z_k - z_c) f_{ky}] \\ M_y + \sum_{k=1}^{k_b} [(z_k - z_c) f_{kx} - (x_k - x_c) f_{kz}] \\ M_z + \sum_{k=1}^{k_b} [(x_k - x_c) f_{ky} - (y_k - y_c) f_{kx}] \end{Bmatrix} \quad (27)$$

If  $\mathbf{J}^O$  is considered to be constant during the short time interval  $\Delta t$ , differentiating Eq. (23)

yields

$$\dot{\mathbf{H}}_C^O = \mathbf{J}^O \dot{\boldsymbol{\omega}}^O \quad (28)$$

Substituting Eq. (28) into Eq. (27) gives

$$\mathbf{J}^O \begin{Bmatrix} \dot{\omega}_x \\ \dot{\omega}_y \\ \dot{\omega}_z \end{Bmatrix} = \begin{Bmatrix} M_x + \sum_{k=1}^{k_b} [(y_k - y_c) f_{kz} - (z_k - z_c) f_{ky}] \\ M_y + \sum_{k=1}^{k_b} [(z_k - z_c) f_{kx} - (x_k - x_c) f_{kz}] \\ M_z + \sum_{k=1}^{k_b} [(x_k - x_c) f_{ky} - (y_k - y_c) f_{kx}] \end{Bmatrix} \quad (29)$$

Combining Eq. (22) with Eq. (29) yields

$$\mathbf{M}_b \mathbf{a}_c = \mathbf{F} + \mathbf{G} \mathbf{f}_b \quad (30)$$

where  $\mathbf{a}_c$  is the centroid acceleration vector of the rigid body, including both translational and angular accelerations.  $\mathbf{M}_b$  is the matrix comprising  $m$  and  $\mathbf{J}^O$ ,  $\mathbf{f}_b$  is the force vector consisting of all the nodal forces. According to Eqs. (11) and (14), matrix  $\mathbf{G}$  in Eq. (30) yields

$$\mathbf{G} = \mathbf{H}^T \quad (31)$$

If  $\mathbf{H}$  is considered to be constant during the short time interval  $\Delta t$ , differentiating and solving Eq. (12) give

$$\mathbf{a}_c = \mathbf{H}^+ \mathbf{a}_b \quad (32)$$

where  $\mathbf{a}_b$  is the nodal acceleration vector of the rigid body.

Substituting Eq. (32) into Eq. (30) gives

$$\overline{\mathbf{M}}_b \mathbf{a}_b = \mathbf{f}_b + \mathbf{G}^+ \mathbf{F} \quad (33)$$

where

$$\overline{\mathbf{M}}_b = \mathbf{G}^+ \mathbf{M}_b \mathbf{H}^+ = (\mathbf{H}^+)^T \mathbf{M}_b \mathbf{H}^+ = \overline{\mathbf{M}}_b^T \quad (34)$$

Eq. (33) is the equation of motion for the rigid body, in which the accelerations of the nodes are used instead of the translational and rotational accelerations of the rigid body.  $\overline{\mathbf{M}}_b$  is the general mass matrix of the rigid body. If only the nodal forces are taken into account, Eq. (33) can be rewritten as

$$\overline{\mathbf{M}}_b \mathbf{a}_b = \mathbf{f}_b \quad (35)$$

### 3. Dynamic analysis of a multibody system

Consider a multibody system composed of  $s_a$  rigid bars and  $s_b$  rigid bodies. The bars and the

rigid bodies are connected by ideal pin joints. After writing Eq. (3) for each of the bars and Eq. (15) for each of the rigid bodies and collecting them into one equation, we obtain the first-order displacement constraint equation, Eq. (36). Similarly, the second-order displacement constraint equation, Eq. (37), is obtained from Eqs. (4) and (20).

$$\mathbf{A}\mathbf{d} = \mathbf{0} \quad (36)$$

$$\mathbf{A}\dot{\mathbf{d}} + \ddot{\mathbf{\Phi}} = \mathbf{0} \quad (37)$$

where  $\mathbf{d}$  is the nodal displacement vector,  $\mathbf{A}$  is an  $s \times n$  matrix,  $n$  is the total nodal degrees of freedom of the multibody system, and  $s$  is calculated according to Eq. (38).

$$s = s_a + 3 \sum_{b=1}^{s_b} k_b \quad (38)$$

Writing Eq. (6) for each of the bars and Eq. (35) for each of the rigid bodies and collecting them into one equation gives

$$\mathbf{M}\mathbf{a} = \mathbf{f} \quad (39)$$

Eq. (39) is the equation of motion of the multibody system.  $\mathbf{M}$  is the total mass matrix, which is the combination of the mass matrices of the bars and those of the rigid bodies.  $\mathbf{a}$  is the nodal acceleration vector, and  $\mathbf{f}$  is the nodal external force vector. Dynamic analysis can be performed by solving Eq. (39) and using the constraints given in Eqs. (36) and (37).

The non-zero solution to Eq. (36) can be expressed as (Tanaka and Hangai 1986, Pellegrino and Calladine 1986)

$$\mathbf{d} = \alpha_1 \mathbf{u}_1 + \alpha_2 \mathbf{u}_2 + \dots + \alpha_p \mathbf{u}_p = \mathbf{U}\boldsymbol{\alpha} \quad (40)$$

where  $\mathbf{u}_1, \mathbf{u}_2, \dots, \mathbf{u}_p$  are independent orthogonal vectors, and called independent modes of the rigid body displacement of the multibody system. They represent the null space orthogonal basis of matrix  $\mathbf{A}$ .  $p = n - \text{rank}(\mathbf{A})$  is the number of rigid body displacement modes,  $n$  is the number of nodal degrees of freedom, and  $\boldsymbol{\alpha}$  is the vector that consisting of  $\alpha_1, \alpha_2, \dots, \alpha_p$ .

In order to solve Eq. (39) numerically, the incremental equation is formulated that can be used for numerical integration method such as Newmark- $\beta$  method. In a short time interval  $t \sim t + \Delta t$ , the displacement considering the first-order term during  $t \sim t + \Delta t$  can be expressed as

$$\mathbf{d}_{t \sim t + \Delta t} = \mathbf{U}_t (\boldsymbol{\alpha}_{t + \Delta t} - \boldsymbol{\alpha}_t) \quad (41)$$

In Eq. (41), the subscripts are used to specify the time interval and the instant. Solving Eq. (37) leads to

$$\dot{\mathbf{d}}_{t \sim t + \Delta t} = -\mathbf{A}_t^+ \ddot{\mathbf{\Phi}}_t \quad (42)$$

where  $\mathbf{A}_t^+$  is the Moore-Penrose generalized inverse matrix of  $\mathbf{A}_t$  at time  $t$ . Eq. (42) can be rewritten as

$$\dot{\mathbf{d}}_{t + \Delta t} - \dot{\mathbf{d}}_t = -\mathbf{A}_t^+ \ddot{\mathbf{\Phi}}_t \quad (43)$$

Consider the Taylor expansion of  $\mathbf{d}_{t + \Delta t}$  with the third-order and higher-order terms ignored

$$\mathbf{d}_{t + \Delta t} = \mathbf{d}_t + \dot{\mathbf{d}}_t \Delta t + \frac{1}{2} \ddot{\mathbf{d}}_t (\Delta t)^2 \quad (44)$$

The displacement increment, including the second-order term, during the interval  $t \sim t + \Delta t$ , can be obtained by substituting Eqs. (41) and (43) into Eq. (44)

$$\mathbf{d}_{t \sim t + \Delta t} = \mathbf{U}_t (\boldsymbol{\alpha}_{t + \Delta t} - \boldsymbol{\alpha}_t) - \frac{1}{2} \mathbf{A}_t^+ \ddot{\boldsymbol{\Phi}}_t \Delta t \quad (45)$$

where  $\dot{\mathbf{d}}_t \Delta t = \mathbf{d}_{t \sim t + \Delta t}$  and  $\ddot{\mathbf{d}}_t \Delta t = \dot{\mathbf{d}}_{t + \Delta t} - \dot{\mathbf{d}}_t$  are used.

In Eq. (45),  $\ddot{\boldsymbol{\Phi}}_t$  can be calculated using Eqs. (5) and (21). For rigid bar  $a$ ,  $\ddot{\boldsymbol{\Phi}}_{a,t} \Delta t$  can be expressed as

$$\begin{aligned} \ddot{\boldsymbol{\Phi}}_{a,t} \Delta t &= \frac{1}{l} (\dot{\mathbf{x}}_j - \dot{\mathbf{x}}_i)^T (\dot{\mathbf{x}}_j - \dot{\mathbf{x}}_i)_t (\Delta t)^2 \\ &= \frac{1}{l} (\mathbf{d}_{j,t \sim t + \Delta t} - \mathbf{d}_{i,t \sim t + \Delta t})^T (\mathbf{d}_{j,t \sim t + \Delta t} - \mathbf{d}_{i,t \sim t + \Delta t}) \end{aligned} \quad (46)$$

where  $\mathbf{d}_{i,t \sim t + \Delta t}$  and  $\mathbf{d}_{j,t \sim t + \Delta t}$  are the first-order displacement increments of the nodes of the rigid bar during the interval  $\Delta t$ , which can be solved according to Eq. (41).

For rigid body  $b$ ,  $\ddot{\boldsymbol{\Phi}}_{b,t} \Delta t$  can be expressed as

$$\begin{aligned} \ddot{\boldsymbol{\Phi}}_{b,t} \Delta t &= -[\mathbf{I} - \mathbf{H}_t \mathbf{H}_t^+] \dot{\mathbf{H}}_t \mathbf{H}_t^+ \mathbf{d}_{b,t \sim t + \Delta t} \Delta t \\ &= -[\mathbf{I} - \mathbf{H}_t \mathbf{H}_t^+] (\dot{\mathbf{H}}_t \Delta t) \mathbf{H}_t^+ \mathbf{d}_{b,t \sim t + \Delta t} \end{aligned} \quad (47)$$

where

$$\dot{\mathbf{H}}_t \Delta t = \{\dot{\mathbf{H}}_{1,t} \Delta t, \dots, \dot{\mathbf{H}}_{k_b,t} \Delta t\}^T \quad (48)$$

$$\begin{aligned} &\dot{\mathbf{H}}_{k,t} \Delta t \\ &= \begin{bmatrix} 0 & 0 & 0 & 0 & \dot{z}_{k,t} - \dot{z}_{c,t} & -(\dot{y}_{k,t} - \dot{y}_{c,t}) \\ 0 & 0 & 0 & -(\dot{z}_{k,t} - \dot{z}_{c,t}) & 0 & \dot{x}_{k,t} - \dot{x}_{c,t} \\ 0 & 0 & 0 & \dot{y}_{k,t} - \dot{y}_{c,t} & -(\dot{x}_{k,t} - \dot{x}_{c,t}) & 0 \end{bmatrix} \Delta t \\ &= \begin{bmatrix} 0 & 0 & 0 & 0 & d_{kz,t \sim t + \Delta t} - d_{cz,t \sim t + \Delta t} & -(d_{ky,t \sim t + \Delta t} - d_{cy,t \sim t + \Delta t}) \\ 0 & 0 & 0 & -(d_{kz,t \sim t + \Delta t} - d_{cz,t \sim t + \Delta t}) & 0 & d_{kx,t \sim t + \Delta t} - d_{cx,t \sim t + \Delta t} \\ 0 & 0 & 0 & d_{ky,t \sim t + \Delta t} - d_{cy,t \sim t + \Delta t} & -(d_{kx,t \sim t + \Delta t} - d_{cx,t \sim t + \Delta t}) & 0 \end{bmatrix} \\ &(k = 1, 2, \dots, k_b) \end{aligned} \quad (49)$$

$d_{kx,t \sim t + \Delta t}$  and the similar displacement terms are the first-order displacement increments of the nodes of the rigid body during the interval  $\Delta t$ , which can be solved according to Eq. (41).

If Eq. (46) is applied to each of the bars, and Eq. (47) is applied to each of the rigid bodies, then the displacement increment, including the second-order term, during the interval  $t \sim t + \Delta t$  can be obtained by substituting Eqs. (46) and (47) into Eq. (45).

The velocity is considered as the time derivative of displacement, which is obtained from  $\dot{\mathbf{d}}_t = \mathbf{d}_{t \sim t + \Delta t} / \Delta t$ . By means of Eq. (45), the velocity and acceleration at time  $t$  can be expressed as

$$\mathbf{v}_t = \mathbf{U}_t \dot{\mathbf{a}}_t - \frac{1}{2} \mathbf{A}_t^+ \ddot{\Phi}_t \quad (50)$$

$$\mathbf{a}_t = \frac{\mathbf{U}_{t+\Delta t} \dot{\mathbf{a}}_{t+\Delta t} - \mathbf{U}_t \dot{\mathbf{a}}_t - \frac{1}{2} (\mathbf{A}_{t+\Delta t}^+ \ddot{\Phi}_{t+\Delta t} - \mathbf{A}_t^+ \ddot{\Phi}_t)}{\Delta t} \quad (51)$$

Substituting Eq. (51) into Eq. (39) and multiplying the equation by  $\mathbf{U}_{t+\Delta t}^T$  on both sides, we obtain

$$\mathbf{U}_{t+\Delta t}^T \mathbf{M}_t \mathbf{U}_{t+\Delta t} \dot{\mathbf{a}}_{t+\Delta t} - \mathbf{U}_{t+\Delta t}^T \mathbf{M}_t \mathbf{U}_t \dot{\mathbf{a}}_t - \frac{1}{2} \mathbf{U}_{t+\Delta t}^T \mathbf{M}_t (\mathbf{A}_{t+\Delta t}^+ \ddot{\Phi}_{t+\Delta t} - \mathbf{A}_t^+ \ddot{\Phi}_t) = \mathbf{U}_{t+\Delta t}^T \mathbf{f}_t \Delta t \quad (52)$$

Eq. (52) can be solved using numerical methods such as the Newmark- $\beta$  method (Bathe and Wilson 1976), which is employed in this paper. According to the Newmark- $\beta$  method, the velocity and the displacement at time  $t+\Delta t$  can be expressed as

$$\dot{\mathbf{a}}_{t+\Delta t} = \dot{\mathbf{a}}_t + \ddot{\mathbf{a}}_t (1-\gamma) \Delta t + \ddot{\mathbf{a}}_{t+\Delta t} \gamma \Delta t \quad (53)$$

$$\mathbf{a}_{t+\Delta t} = \mathbf{a}_t + \dot{\mathbf{a}}_t \Delta t + \ddot{\mathbf{a}}_t \left( \frac{1}{2} - \beta \right) (\Delta t)^2 + \ddot{\mathbf{a}}_{t+\Delta t} \beta (\Delta t)^2 \quad (54)$$

where  $\beta$  and  $\gamma$  are two parameters used in the calculation, and they are set to  $\beta=0.25$  and  $\gamma=0.5$  in this research. From Eqs. (53) and (54), we have

$$\ddot{\mathbf{a}}_{t+\Delta t} = \frac{\mathbf{a}_{t+\Delta t} - \mathbf{a}_t}{\beta (\Delta t)^2} - \frac{\dot{\mathbf{a}}_t}{\beta \Delta t} - \left( \frac{1}{2\beta} - 1 \right) \ddot{\mathbf{a}}_t \quad (55)$$

$$\dot{\mathbf{a}}_{t+\Delta t} = \frac{\gamma}{\beta \Delta t} (\mathbf{a}_{t+\Delta t} - \mathbf{a}_t) + \left( 1 - \frac{\gamma}{\beta} \right) \dot{\mathbf{a}}_t + \left( 1 - \frac{\gamma}{2\beta} \right) \ddot{\mathbf{a}}_t \Delta t \quad (56)$$

Substituting Eq. (56) into Eq. (52) yields

$$\begin{aligned} & \mathbf{U}_{t+\Delta t}^T \mathbf{M}_t \mathbf{U}_{t+\Delta t} \frac{\gamma}{\beta \Delta t} \mathbf{a}_{t+\Delta t} \\ &= \mathbf{U}_{t+\Delta t}^T \mathbf{f}_t \Delta t + \mathbf{U}_{t+\Delta t}^T \mathbf{M}_t \mathbf{U}_{t+\Delta t} \left[ \frac{\gamma}{\beta \Delta t} \mathbf{a}_t - \left( 1 - \frac{\gamma}{\beta} \right) \dot{\mathbf{a}}_t - \left( 1 - \frac{\gamma}{2\beta} \right) \ddot{\mathbf{a}}_t \Delta t \right] \\ & \quad + \mathbf{U}_{t+\Delta t}^T \mathbf{M}_t \mathbf{U}_t \dot{\mathbf{a}}_t + \frac{1}{2} \mathbf{U}_{t+\Delta t}^T \mathbf{M}_t (\mathbf{A}_{t+\Delta t}^+ \ddot{\Phi}_{t+\Delta t} - \mathbf{A}_t^+ \ddot{\Phi}_t) \end{aligned} \quad (57)$$

Eq. (57) is the dynamic iterative formula expressed using the vector  $\mathbf{a}$ . The number of variables in Eq. (57) is  $p$ , which is less than the number of variables in Eq. (39).

$\mathbf{a}_{t+\Delta t}$  can be solved iteratively for the time interval  $t \sim t+\Delta t$  using Eq. (57), and  $\ddot{\mathbf{a}}_{t+\Delta t}$  and  $\dot{\mathbf{a}}_{t+\Delta t}$  can be obtained from Eqs. (55) and (56). The nodal displacements are obtained by substituting  $\mathbf{a}_{t+\Delta t}$  into Eq. (45), and the nodal velocities and accelerations are obtained by the numerical differentiation of the displacements. The centroid displacement vector of the rigid body,  $\{D_x D_y D_z \omega_x \Delta t \omega_y \Delta t \omega_z \Delta t\}^T$ , is obtained from Eq. (19), and the centroid coordinates with respect to the fixed reference system are updated accordingly. The Euler angle increments for the time interval

$t \sim t + \Delta t$  are obtained from Eq. (58), and the Euler angles of the rigid body are updated accordingly. The inertia matrix at instant  $t + \Delta t$  is obtained next by substituting the updated Euler angles into Eqs. (25) and (24), and the mass matrix is updated accordingly so that  $\mathbf{a}$ ,  $\dot{\mathbf{a}}$  and  $\ddot{\mathbf{a}}$  can be obtained from Eq. (57) at the next time step. The nodal displacements, velocities and accelerations are obtained similarly at each time step.

$$\begin{Bmatrix} \dot{\psi} \\ \dot{\theta} \\ \dot{\phi} \end{Bmatrix} \Delta t = \begin{bmatrix} -\sin\psi \cot\theta & \cos\psi \cot\theta & 1 \\ \cos\psi & \sin\psi & 0 \\ \frac{\sin\psi}{\sin\theta} & -\frac{\cos\psi}{\sin\theta} & 0 \end{bmatrix} \begin{Bmatrix} \omega_x \\ \omega_y \\ \omega_z \end{Bmatrix} \Delta t \quad (58)$$

#### 4. Numerical examples

A computer program was written for implementing the proposed method (the flowcharts are shown in Appendices A and B), and a five-bar linkage model was firstly analyzed using the program. The numerical results are compared with the results of the numerical integration of the equations obtained using the Lagrange multiplier method. Dynamic analysis results of two deployable structures using the proposed method are also compared with those using the commercial software package ADAMS (MSC.ADAMS 2005), in which the Lagrange multiplier method is implemented.

##### 4.1 A five-bar linkage

The five-bar linkage in Fig. 5 is a two-degree-of-freedom system. The masses and the lengths of the bars are the same with  $m_{AB}=m_{BC}=m_{CD}=m_{DE}=2.45076$  kg and  $l_{AB}=l_{BC}=l_{CD}=l_{DE}=1$  m. The distance between the fixed points  $A$  and  $E$  is 2 m. The linkage starts to move under its self-weight with initial conditions  $x_C=1.0$  m,  $y_C=0.0$  and  $v_{Cx}=v_{Cy}=0$  as shown in Fig. 5. In this example, the lumped mass matrix is used in the proposed method. For the Lagrange multiplier method, the masses of bars are replaced by the centralized masses at nodes  $B$ ,  $C$  and  $D$ . The time history of  $x_B$  and  $v_{Bx}$  calculated using the proposed method and the Lagrange multiplier method is shown in Fig. 6. The same results are obtained from the two methods.

##### 4.2 A deployable reflector with stiff panels

Fig. 7 shows a stiff-panel reflector similar to the reflector proposed by Rogers *et al.* (1993). The reflector is composed of four stiff panels, forty-one rigid bars and eight cables. To deploy the reflector synchronously, fourteen synchronous gears are located at nodes 2~8 and nodes 11~17. By shortening the length of the cables through motors, the deployable reflector can be stowed from the fully deployed state. As shown in Fig. 7(a), the four stiff panels are of the same size,  $2.0 \text{ m} \times 1.0$  m. As shown in Fig. 7(b), the diagonal rigid bars have the same length of 1.5 m, and the length of the other rigid bars is 1.0 m. To simplify the calculation, the cables are replaced by eight pairs of forces in the deployment analysis. The magnitude of the forces is maintained at a constant level of 50.0 N along the direction of the cables. The synchronous gears are considered as the constraint condition, where the rotation angles of gears are kept the same during the folding process. The gravity of the reflector is not considered in the analysis.

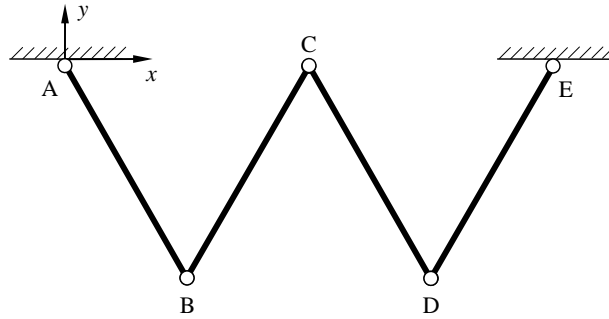
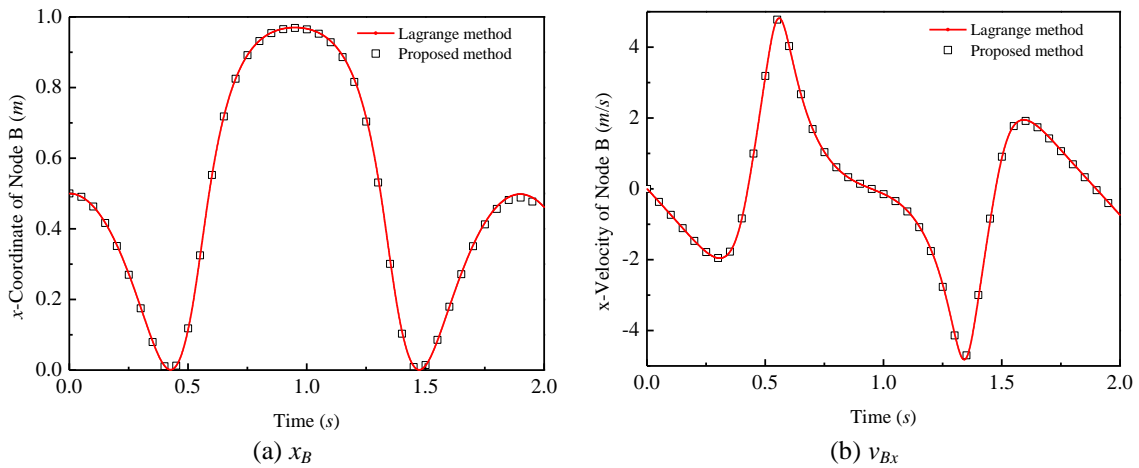


Fig. 5 A five-bar linkage

Fig. 6 Time history of  $x_B$  and  $v_{Bx}$ 

The dynamic process is analyzed starting from the fully deployed configuration and ending at the predetermined folded configuration. The displacements and velocities are initially set to zero, and the folding process is simulated using both the proposed method and the ADAMS software package (MSC.ADAMS 2005). Fig. 8 shows the change in the shape of the reflector during the folding process. The reflector reaches the predetermined configuration when  $t$  equals 9.07 s. In Fig. 9, the  $x$  and  $y$  components of the coordinates, velocities and accelerations of node 5 are plotted from the simulation results. The time interval  $\Delta t$  used in both the proposed method and ADAMS was  $1.0 \times 10^{-2}$  s. The simulation results from the two methods are almost the same.

The number of unknowns in the dynamic equations in the proposed method is the number of independent rigid body displacement modes, which equals six in this numerical model. Comparatively, the degree of freedom (DOF) of this numerical model in ADAMS equals 47 (The numerical model comprises 45 moving parts, 76 spherical joints, 14 general constraints and 19 redundant constraint equations, so  $\text{DOF} = 45 \times 6 - 76 \times 3 - 14 + 19 = 47$ ). Comparison of the computational efficiency between the proposed method and ADAMS is shown in Table 1. It can be seen from Table 1 that the analysis using the proposed method takes as little as approximately one-half the CPU time of that required by ADAMS when the two methods give the same high accuracy.

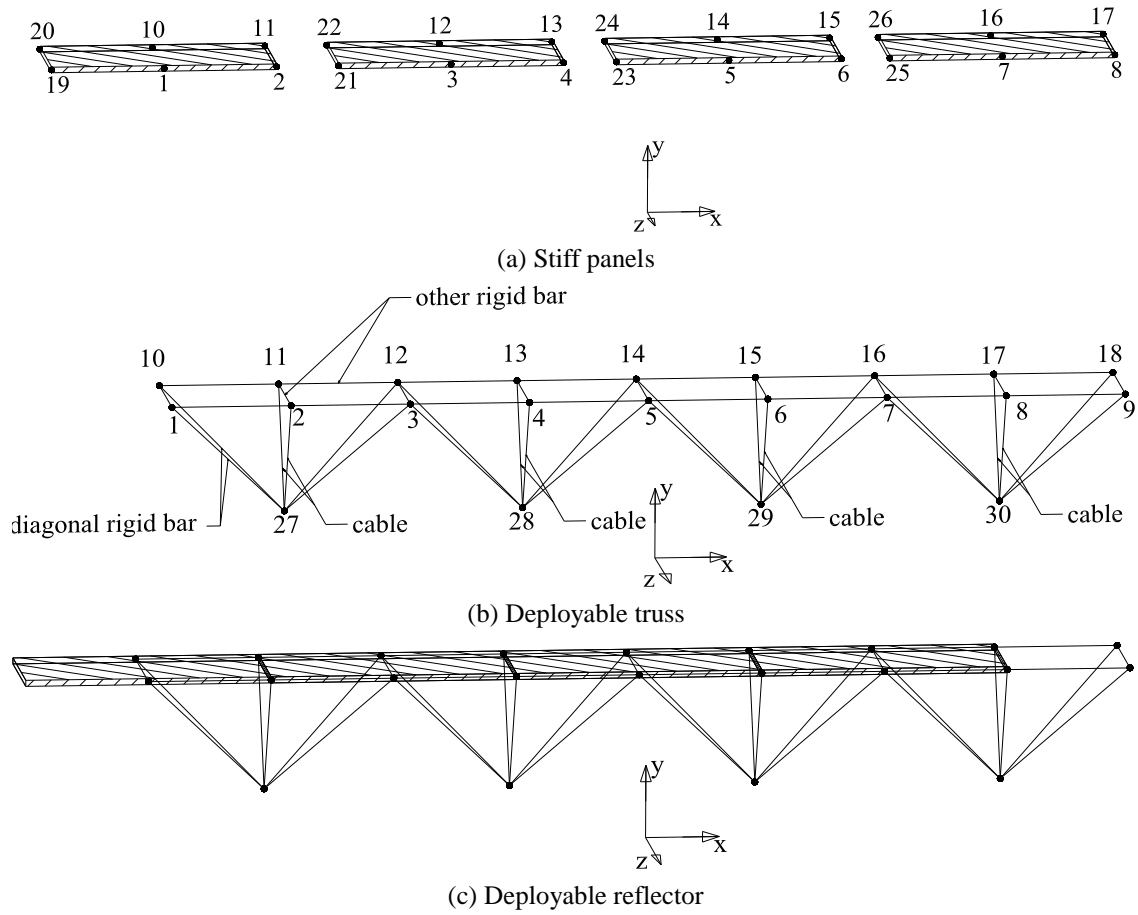


Fig. 7 A deployable reflector with stiff panels

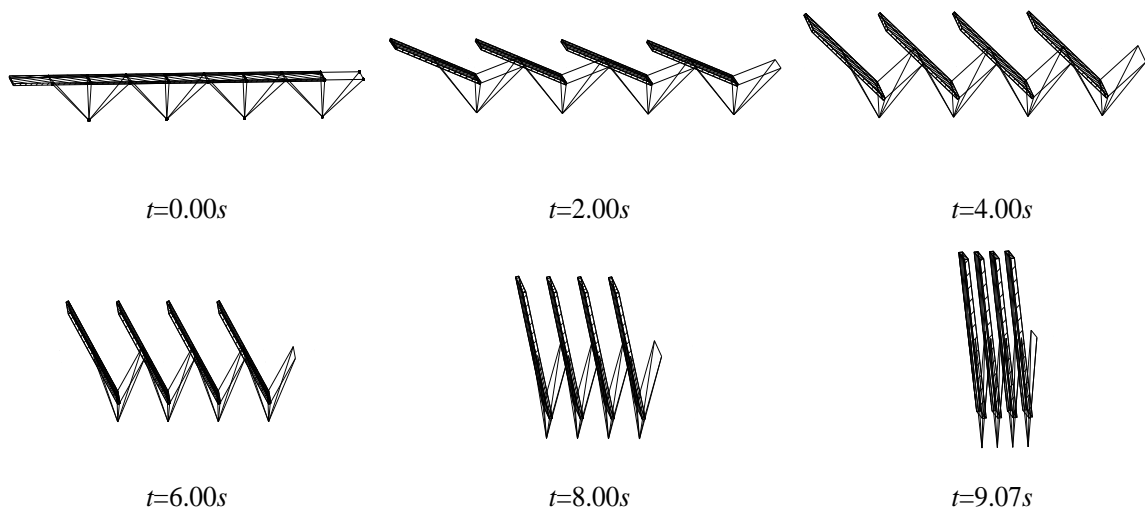


Fig. 8 Simulation of folding process

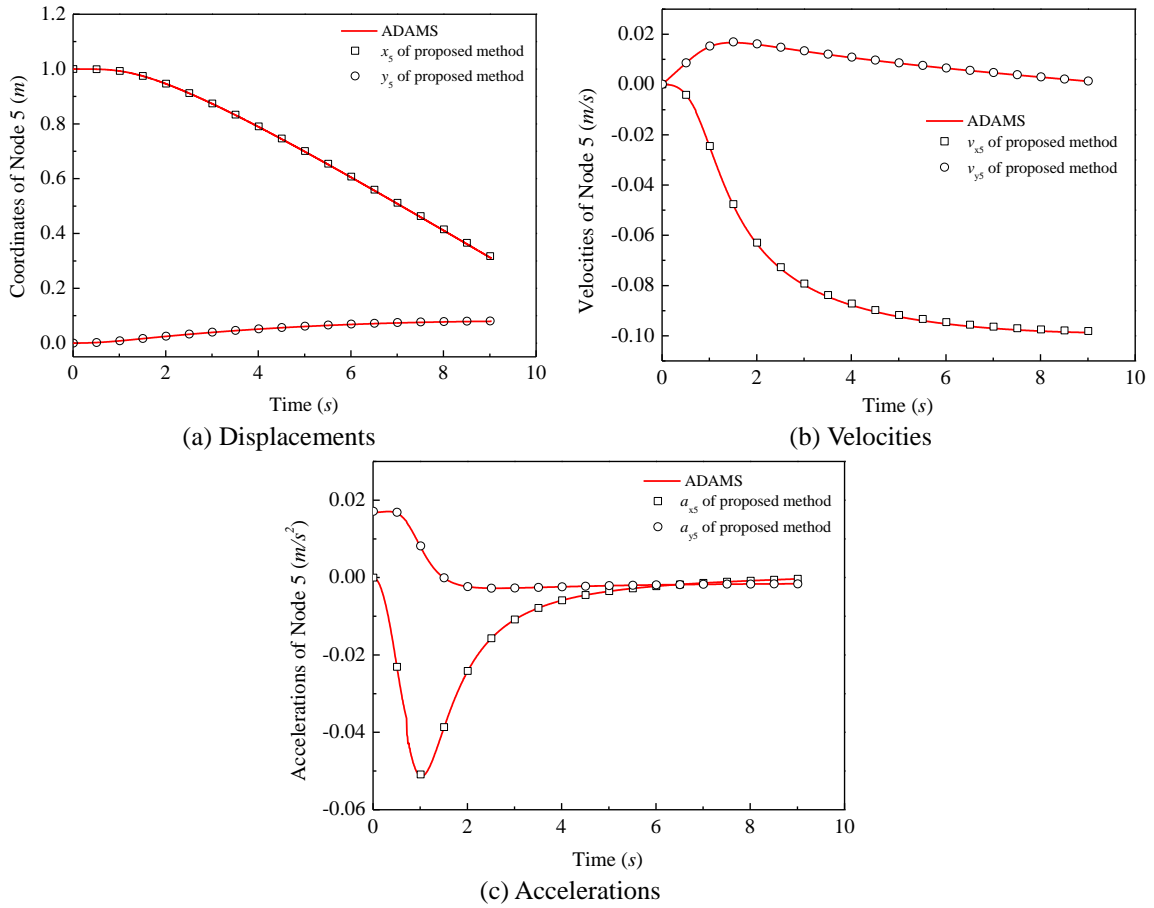


Fig. 9 Time histories of dynamic responses of node 5

Table 1 Computational efficiency comparison of Example 2

Time interval $\Delta t$ (s)	Computing time (s) (present paper)	Computing time (s) (ADAMS)	Accuracy
$1.00 \times 10^{-3}$	76.14	252	high (present paper) low (ADAMS)
$1.00 \times 10^{-2}$	7.84	15	high
$2.00 \times 10^{-2}$	3.86	7	high
$1.00 \times 10^{-1}$	—*	2	— (present paper) very low (ADAMS)

\*symbol-in the table means calculation failed.

### 4.3 A deployable truss

Fig. 10 shows a three-dimensional deployable truss used in deployable reflectors (Thomson 1999). The truss consists of thirty rigid bars and a continuous diagonal cable. The deployable truss

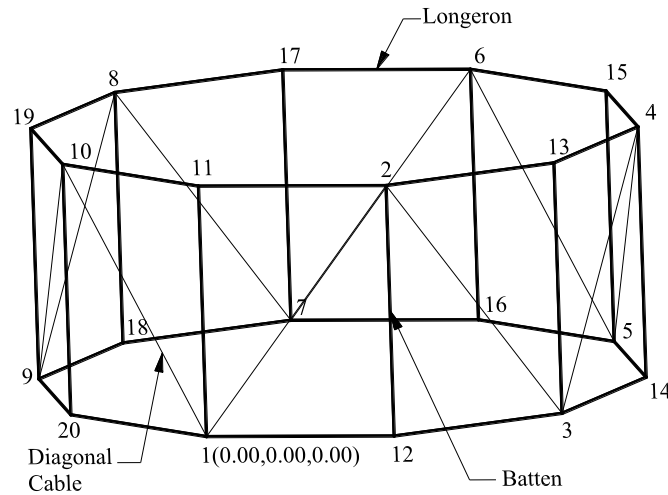


Fig. 10 A deployable truss

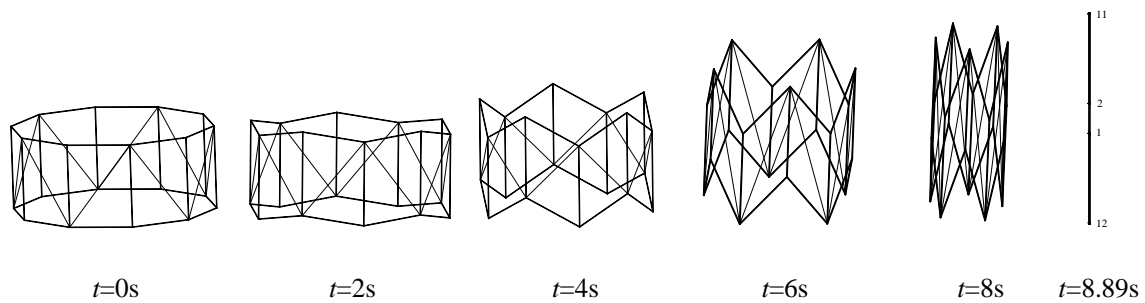


Fig. 11 Simulation of folding process

is stowed by shortening the length of the cable (for example, using a motor). In the fully deployed state, the deployable truss is 1.6 m high, and the upper and lower truss rings are in the shape of a decagon with edges of length 1.2 m. The density of the truss members is 9.8 kg/m. In the deployment analysis, the continuous cable is replaced by ten pairs of forces. The magnitude of the forces is maintained at a constant level of 2.0 N along the direction of the diagonal cable. The gravity of the truss is not considered in the analysis.

The dynamic process is analyzed from the fully deployed configuration to the fully folded configuration using both the proposed method and ADAMS. The displacements and velocities are initially set to zero. Fig. 11 shows the configurations of the truss at different instants during the folding process. The deployable truss is completely stowed when  $t$  equals 8.890 s. Fig. 12 gives the simulated coordinates, velocities and accelerations of node 1. The time interval  $\Delta t$  employed in both the proposed method and ADAMS was  $1.0 \times 10^{-2}$  s, and the two methods give almost the same simulation results.

The number of unknowns in the dynamic equations of the proposed method is the number of independent rigid body displacement modes, which equals eleven in this numerical model. Comparatively, the degree of freedom (DOF) of this numerical model in ADAMS equals 45 (This

numerical model comprises 30 moving parts, 10 planar joints, 40 spherical joints and 15 redundant constraint equations, so  $DOF=30 \times 6 - 10 \times 3 - 40 \times 3 + 15 = 45$ ). The computational efficiencies of the proposed method and ADAMS are compared in Table 2, indicating that the proposed method takes approximately one-sixth of the CPU time required by ADAMS when the same high accuracy is achieved.

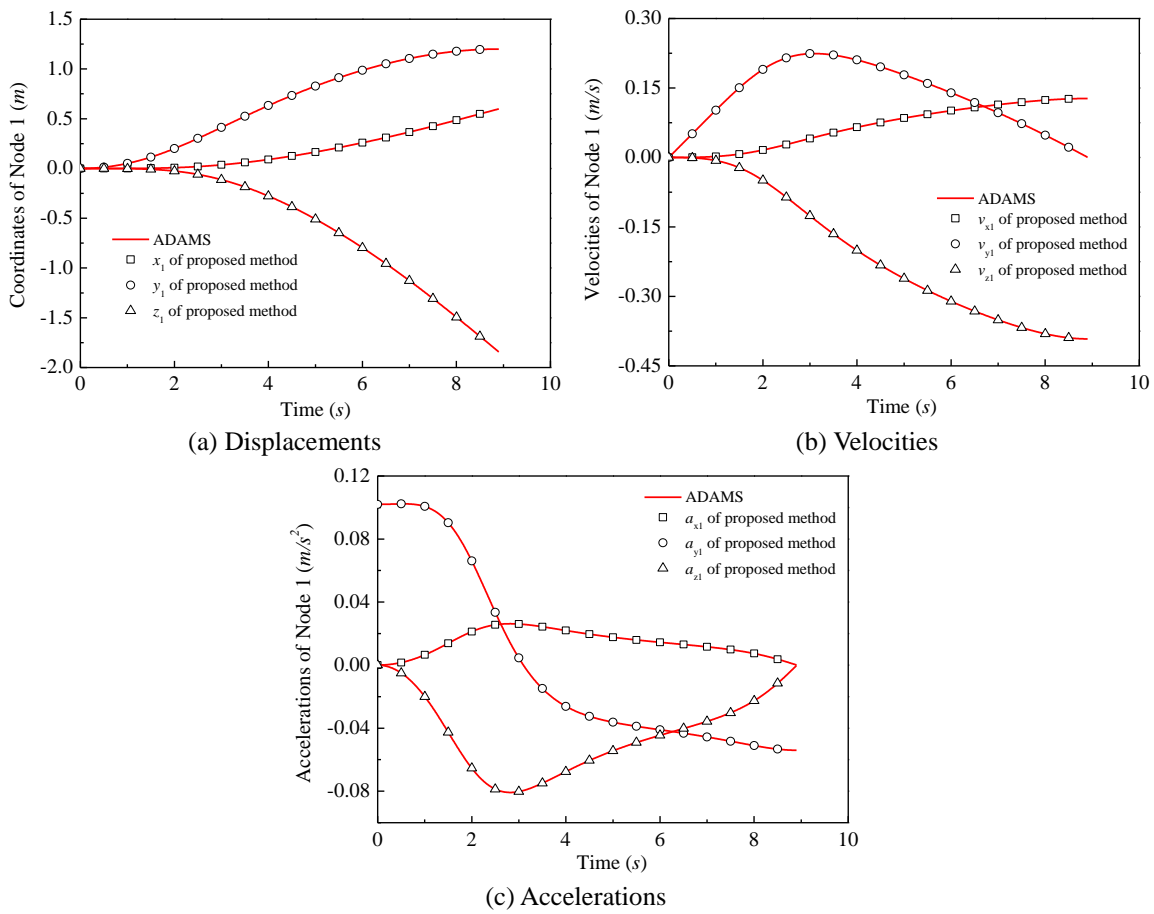


Fig. 12 Time histories of dynamic responses of node 1

Table 2 Computational efficiency comparison of Example 3

Time interval $\Delta t$ (s)	Computing time (s) (present paper)	Computing time (s) (ADAMS)	Accuracy
$1.00 \times 10^{-4}$	321.50	–	high (present paper) – (ADAMS)
$1.00 \times 10^{-3}$	32.27	238	high
$1.00 \times 10^{-2}$	3.25	18	high
$1.00 \times 10^{-1}$	–*	–	–

\* symbol – in the table means calculation failed.

## 5. Conclusions

Multibody dynamic analysis based on an inertial coordinate system has many advantages, such as clarity of the resulting formulation, convenience for computer processing and ease of integrating the analysis with finite element modeling and continuum mechanics theory. It has become an effective method of dynamic analysis for multibody systems. This paper proposed a new dynamic analysis method based on nodal Cartesian coordinates, where a generalized inverse matrix method is applied to analysis of multibody dynamics. The constraint equations of displacements and the equations of motion using displacement modes as variables are established by means of Moore-Penrose generalized inverse matrix. The method proposed in this paper has less unknowns and a simple formulation.

Three representative numerical examples were analyzed using the proposed method, and the results were also compared with other analysis methods, through which the validity and efficiency of the proposed method are demonstrated.

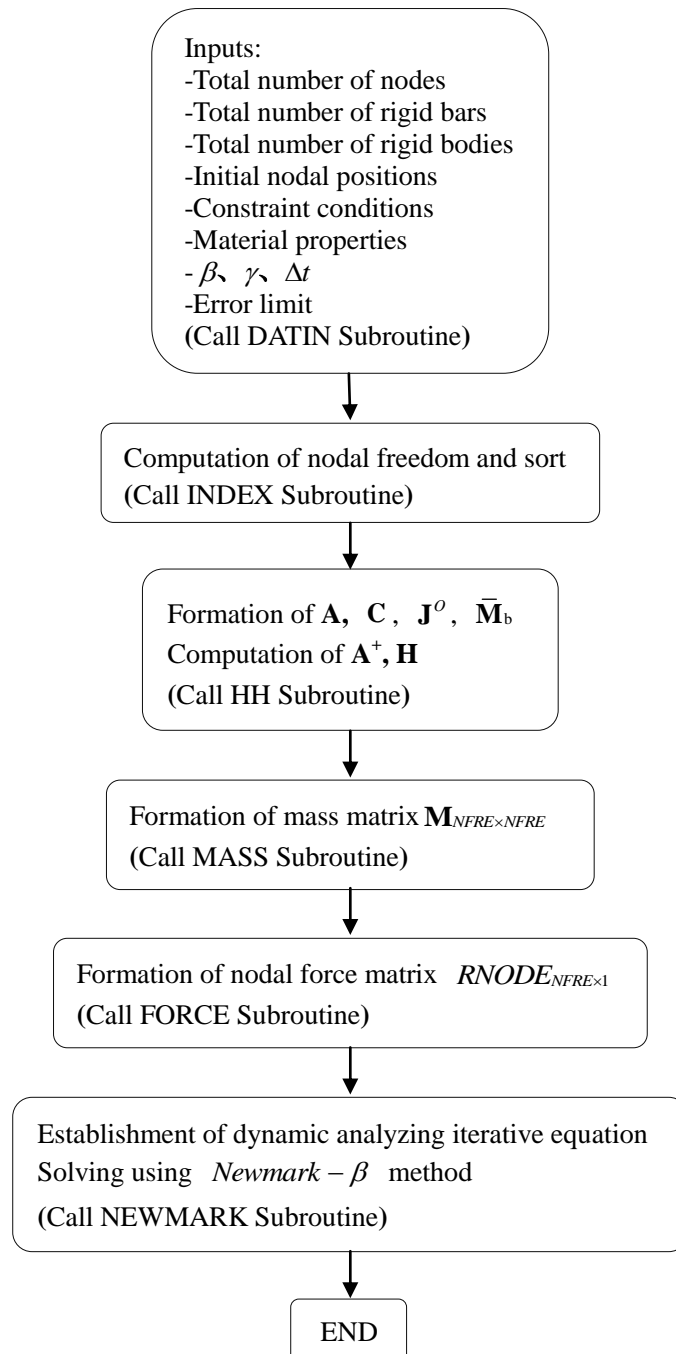
The second-order displacement constraint equation is also formulated in this paper. Since the generalized inverse of the large dimension matrix  $\mathbf{A}$  should be calculated when the second-order term is considered, the efficiency of numerical calculation is expected to be further investigated in future study.

## References

- Ahmed, A.S. (2013), *Dynamics of Multibody Systems*, Fourth Edition, Cambridge University Press, Chicago, USA.
- Bathe, K.J. and Wilson, E.L. (1976), *Numerical Methods in Finite Element Analysis*, Prentice-Hall, New Jersey.
- Ben-Israel, A. and Greville, T.N.E. (2003), *Generalized Inverses: Theory and Applications*, Springer-Verlag, New York.
- Çelik, E. and Bayram, M. (2004), "Numerical solution of differential-algebraic equation systems and applications", *Appl. Math. Comput.*, **154**, 405-413.
- Elsheikh, A. (2015), "An equation-based algorithmic differentiation technique for differential algebraic equations", *J. Comput. Appl. Math.*, **281**, 135-151.
- Gan, B.S., Trinh, T.H., Le, T.H. and Nguyen, D.K. (2015), "Dynamic response of non-uniform Timoshenko beams made of axially FGM subjected to multiple moving point loads", *Struct. Eng. Mech.*, **53**(5), 981-995.
- García de Jalón, J., Unda, J. and Avello, Al. (1986), "Natural coordinates for the computer analysis of three dimensional multibody systems", *Comput. Meth. Appl. Mech. Eng.*, **56**(3), 309-327.
- García de Jalón, J. and Bayo, E. (1993), *Kinematic and Dynamic Simulation of Multibody Systems-the Real-Time Challenge*, Springer, New York.
- García de Jalón, J. (2007), "Twenty-five years of natural coordinates", *Multibody Syst. Dyn.*, **18**(1), 15-33.
- Hangai, Y. and Kawaguchi, K. (1990), "Analysis for shape-finding process of unstable link structures", *Bull. IASS*, **30**(100), 116-128.
- Hangai, Y. and Wu, M. (1999), "Analytical method of structural behaviors of a hybrid structure consisting of cables and rigid structures", *Eng. Struct.*, **21**(8), 726-736.
- Ider, S.K. and Amirouche, F.M. (1988), "Coordinate reduction in the dynamics of constrained multibody systems-a new approach", *ASME J. Appl. Mech.*, **55**(4), 899-904.
- Kamman, J.W. and Huston, R.L. (1984), "Dynamics of constrained multibody system", *ASME J. Appl. Mech.*, **51**(4), 899-903.

- Kane, T.R. (1961), "Dynamics of nonholonomic systems", *ASME J. Appl. Mech.*, **28**, 574-578.
- Kawaguchi, K., Hangai, Y. and Miyazaki, K. (1993), "The dynamic analysis of kinematically indeterminate frameworks", *Proc. IASS Symposium 1993*, Istanbul.
- Kim, S.S. and Vanderploeg, M.J. (1986), "QR decomposition for state space representation of constrained mechanical dynamic systems", *ASME J. Appl. Mech., Tran. Auto. Des.*, **108**(2), 183-188.
- Liu, C.Q. and Huston, R.L. (2008), "Another form of equations of motion for constrained multibody systems", *Nonlin. Dyn.*, **51**(3), 465-475.
- Masarati, P., Morandini, M. and Fumagalli, A. (2014), "Control constraint of underactuated aerospace systems", *ASME J. Comput. Nonlin. Dyn.*, **9**(2), 021014.
- Montgomery, E. (2004), "Technology advancement for Solar Sail Propulsion (SSP) for NASA science missions to the inner solar system", *A Summary Status Briefing to the Solar Sail Technology & Applications Conference*, September, Greenbelt, Maryland, USA.
- MSC. ADAMS Documentation (2005), MSC Software Corporation.
- Olivier, A.B. and André, L. (2008), "Review of Contemporary Approaches for Constraint Enforcement in Multibody Systems", *ASME J. Comput. Nonlin. Dyn.*, **3**(1), 011005.
- Orlandea, N., Chace, M.A. and Calahan, D.A. (1977), "A sparsity-oriented approach to the dynamic analysis and design of mechanical systems-part I and part II", *J. Manuf. Sci. Eng.*, **99**, 773-784.
- Pellegrino, S. and Calladine, C.R. (1986), "Matrix analysis of statically and kinematically indeterminate frameworks", *Int. J. Solid. Struct.*, **22**(4), 409-428.
- Penrose, R. (1955), "A generalized inverse for matrices", *Proc. Camb. Philos. Soc.*, **51**(3), 406-413.
- Rahnejat, H. and Rothberg S. (2004), *Multi-body Dynamics: Monitoring and Simulation Techniques III*, Professional Engineering Publishing.
- Roberson, R.E. and Schwertassek, R. (1988), *Dynamics of Multibody Systems*, Springer-Verlag, Berlin.
- Rogers, C.A., Stutzman, W.L., Campbell, T.G. and Hedgepeth, J.M. (1993), "Technology assessment and development of large deployable antennas", *J. Aerosp. Eng.*, **6**(1), 34-54.
- Schiehlen, W. (2007), "Multibody system dynamics: roots and perspectives", *Multibody Syst. Dyn.*, **1**, 149-188.
- Singh, R.P. and Likins, P.W. (1985), "Singular value decomposition for constrained dynamical systems", *ASME J. Appl. Mech.*, **52**(4), 943-948.
- Tanaka, H. and Hangai, Y. (1986), "Rigid body displacement and stabilization condition of unstable truss structures", *Proc. IASS Symposium 1986*, Osaka, Elsevier Science Publishers.
- Thomson, M.W. (1999), "The astromesh deployable reflector", *Antennas Propag Soc Int Symp*, **3**, 1516-1519.
- Udwadia, F.E. and Kalaba, R.E. (2001), "Explicit equations of motion for mechanical systems with nonideal constraints", *ASME J. Appl. Mech.*, **68**(3), 462-467.
- Udwadia, F.E., Kalaba, R.E. and Pohomsiri, P. (2004), "Mechanical systems with nonideal constraints: explicit equations without the use of generalized inverses", *ASME J. Appl. Mech.*, **71**(5), 615-621.
- Wittenburg, J. (1977), *Dynamics of Systems of Rigid Bodies*, Teubner B.G., Stuttgart.
- Yesilce, Y. (2015), "Differential transform method and numerical assembly technique for free vibration analysis of the axial-loaded Timoshenko multiple-step Beam carrying a number of intermediate lumped masses and rotary inertias", *Struct. Eng. Mech.*, **53**(3), 537-573.
- Zhao, M. and Guan, F. (2005), "Kinematic analysis of deployable toroidal spatial truss structures for large mesh antenna", *J. IASS*, **46**(149), 195-204.

### Appendix A. Flowchart of the proposed computational procedure



**Appendix B. Flowchart of the iterative solving process**

